Multichannel Wavelet Scheme for Color Image Processing

S. Agreste* and A. Vocaturo†

Department of Mathematics
Messina University, Italy
**sagreste@unime.it*
†avocaturo@unime.it

Every day massive quantities of two-dimensional documents are produced, stored and transmitted. Digital color images are the most prominent type of data in this category. To process these objects a variety of powerful and sophisticated wavelet-based schemes have been developed and implemented.
Considering that digital color images are vector objects with three components, they can be suitably processed in the context of a multichannel Multi Resolution Analysis.
In this work we focus on a new vector approach to multichannel wavelet analysis of color images based on several classes of *full rank* filters, showing the results of a wide experimentation.

Keywords: Multichannel wavelet, digital image processing

1. Introduction

The bulk of information necessary to represent digital objects grows day by day, such as the number of pixel of digital camera or videocamera. So it has become necessary and essential to create image files with manageable and transmittable size. Compression algorithms are used in the standards such as JPEG and MPEG to reduce the number of bits required for representing an image or a video sequence. The wavelet transform has emerged as a cutting edge technology, within the field of image compression. Wavelet based coding provides substantial improvements in picture quality at higher compression ratios. Over the past few years a variety of powerful and sophisticated wavelet-based schemes for image compression have been developed and implemented.

Historically, the concept of wavelets is originated from the study of time-frequency signal analysis, wave propagation, and sampling theory. In 1982,

APPLIED AND INDUSTRIAL MATHEMATICS IN ITALY III - Selected Contributions from the 9th SIMAI Conference

http://www.worldscibooks.com/mathematics/7379.html

Jean Morlet[1,2] first introduced the idea of wavelets as a family of functions constructed by using translation and dilation of a *mother wavelet* for the analysis of nonstationary signals. Today wavelet analysis is an axciting method for solving difficult problems in several disciplines with applications as diverse as data compression, image processing, pattern recognition (Ref. 3,4). Since the early 1990s, multiwavelets have been introduced as generalization of wavelet functions (Ref. 5,6). Multiwavelets with multiplicity r are vector-values functions. A wavelet functions are the scalar case, when the multiplicity $r = 1$.

Unlike the scalar case, some extra degrees of freedom are allowed, which can be used to construct functions with several desirable properties, combining, for example, orthogonality, symmetry, short support and vanishing moments. All these *good properties* are needed for efficiently processing two-dimensional signals, hence multiwavelets are more powerful than wavelet in image processing. In general the application of the multiwavelet decomposition/reconstruction scheme requires two additional steps respect to the scalar case. The first consists in finding from a given set of input data $\{y_1, y_2, ..., y_m\}$, r sequences of initial coefficients $\left\{c_i^{k,0}\right\}_{k \in Z}$, $i = 1, ..., r$, needed by the analysis phase. This step is called *pre-filtering* of the data, since it can be seen as the application of a filter to the initial data. The second step is called *post-filtering*. It consists in finding the output data from a vector of r entries obtained from the synthesis phase.

The multichannel wavelet has been introduced to analysis multichannel signal in Ref. 7,8. In this case the pre and postfiltering steps are not required. This function allows to process a signal with r *vector-valued* signal by means only one decomposition/reconstruction or better that processes the signal as a multichannel signal with possibly intricate correlations between some of these channels. A good example of multichannel signal is a color digital image. In fact because color image has at least three components in according to the color model representation. The color pixels are vectors. In RGB system, each point $\mathbf{c}$ can be interpreted as a vector $\mathbf{c} = [c_R, c_G, c_B]^T$. The components of $\mathbf{c}$ are the RGB components of a color image at a point (Ref. 9).

In this paper we are going to present an innovative denoising and compression algorithm based on multichannel wavelet. The work is organized as follows. We start by presenting the multichannel wavelet theory from Multichannel MultiResolution Analysis point of view and then we present the denoising and compression algorithms. In the last part we expose some experimental results obtained. We have looked over the results with PSNR

APPLIED AND INDUSTRIAL MATHEMATICS IN ITALY III - Selected Contributions from the 9th SIMAI Conference

(Peak Signal to Noise Ratio) and WPSNR (Weight Peak Signal to Noise Ratio) values.

2. Multichannel MultiResolution Analysis and Multichannel Wavelet

In order to model and analyze a multichannel signal we introduce the *Multichannel MultiResolution Analysis* (MMRA). This analysis is based on the concept of *matrix refinable functions* known from the study of *full rank* stationary vector subdivision scheme.[10]

We consider the MMRA like a natural extension of the well-known *multiresolution analysis* to vector valued functions. It is necessary to observe that here we are not considering an MRA with multiplicity, that is, a scalar MRA generated by a finite number of functions instead of a single one. We are interested in a MMRA for the space:

$$L_2(\mathbb{R})^{Z_r} = \left\{ \boldsymbol{f} : \mathbb{R} \to \mathbb{R}^r : \|\boldsymbol{f}\|_2 = \left(\sum_{j \in \mathbb{Z}_r} \int_{\mathbb{R}} |f_j(x)|^2 \, dx \right)^{\frac{1}{2}} < \infty \right\},$$

of square integrable vector fields.
A MMRA is defined by a *nested* sequence of closed subspace $V_0 \subset V_1 \subset \ldots \subset L_2(\mathbb{R})^{\mathbb{Z}_r}$ with the properties that:

- they are *shift invariant*
  $\boldsymbol{f} \in V_k \Leftrightarrow \boldsymbol{f}(\cdot + j) \in V_k, \quad j \in Z$;
- they are *scaled* versions of each other
  $\boldsymbol{f} \in V_0 \Leftrightarrow \boldsymbol{f}(2^k \cdot) \in V_k$;
- the are generated by *stable* integer translates of certain vector fields:
  $V_0 = span \left\{ \boldsymbol{f}_j : j \in \mathbb{Z}_r \right\}$, where the translates of vector fields $\boldsymbol{f}_j, j \in \mathbb{Z}_r$, forms a *Riesz basis* in $L_2(\mathbb{R})^r$ that is,

$$\left\| \sum_{j \in \mathbb{Z}_r} \sum_{k \in \mathbb{Z}} c_{jk} \boldsymbol{f}_j(\cdot - k) \right\|_2 \approx \left(\sum_{j \in \mathbb{Z}_r} \sum_{k \in \mathbb{Z}} |c_{jk}|^2 \right)^{\frac{1}{2}}$$

  Let $\boldsymbol{F} \in L_2(\mathbb{R})^{\mathbb{Z}_r \times \mathbb{Z}_r}$ be the matrix value function with rows $\boldsymbol{f}_j^T$, $j \in \mathbb{Z}_r$ and $\boldsymbol{c}(k)$, $k \in \mathbb{R}^{\mathbb{Z}_r}$ be the vector of entries c_{jk}, $j \in \mathbb{Z}_r$, this condition can be written as $|\boldsymbol{F} * \boldsymbol{c}|_2 \sim |\boldsymbol{c}|_2$.

APPLIED AND INDUSTRIAL MATHEMATICS IN ITALY III - Selected Contributions from the 9th SIMAI Conference

http://www.worldscibooks.com/mathematics/7379.html

Any MMRA is generated by a *matrix refinable* function $\boldsymbol{F} \in L_2(\mathbb{R})^{\mathbb{Z}_r \times \mathbb{Z}_r}$, that is, a function for which there exists a finitely supported *mask*

$$\mathbf{A} = \left(\mathbf{A}(k) \in \mathbb{R}^{\mathbb{Z}_r \times \mathbb{Z}_r} : k \in \mathbb{Z}\right) \in \ell_{00}^{\mathbb{Z}_r \times \mathbb{Z}_r}$$

such that

$$\boldsymbol{F} = (\boldsymbol{F} * \mathbf{A})\,(2\cdot) := \sum_{k \in \mathbb{Z}} \boldsymbol{F}(2 \cdot -k)\mathbf{A}(k). \tag{1}$$

where $*$ symbol represents the *convolution* operator between matrix valued function $\boldsymbol{F}$ and matrix sequences $\boldsymbol{A}$.

Equation 1 is called *matrix refinement equation*. Like in the classical scalar MRA, refinable functions also form the building blocks for the MMRA. The matrix-valued function $\boldsymbol{F} \in L_2(\mathbb{R})^{\mathbb{Z}_r \times \mathbb{Z}_r}$ which generates the MMRA, is called the *scaling function* of the MMRA.

To introduce the relative multichannel wavelet it is necessary to suppose that exists a *wavelet* function for any MMRA generated by an *orthogonal* matrix function, that is, by a matrix function $\boldsymbol{F} \in L_2(\mathbb{R})$ such that:

$$\langle \boldsymbol{F}, \boldsymbol{F}(\cdot - j)\rangle = \delta_{0j}, \quad j \in \mathbb{Z}$$

where $\langle \cdot, \cdot \rangle$ represents the skew symmetric bilinear form

$$\langle \cdot, \cdot \rangle : L_2(\mathbb{R})^{\mathbb{Z}_m \times \mathbb{Z}_k} \times L_2(\mathbb{R})^{\mathbb{Z}_m \times \mathbb{Z}_l} \longrightarrow \mathbb{R}^{\mathbb{Z}_k \times \mathbb{Z}_l}$$

defined as

$$\langle F, G \rangle := \int_{\mathbb{R}} \boldsymbol{F}^T(x)\boldsymbol{G}(x)dx.$$

Since an MMRA consists of a nested sequence of spaces

$$... \subset V_{j-1} \subset V_j \subset V_{j+1} \subset ... \qquad , j \in \mathbb{N}$$

it is possible to define the relative orthogonal complements:

$$W_j := V_{j+1} \ominus V_j, \text{ i.e. } V_{j+1} = V_j \oplus W_j, \quad j \in \mathbb{N}_0$$

Let $\boldsymbol{F} \in V_j$ and let $\mathbf{G} \in W_j$, the orthogonality condition has to be understood in the sense that

$$\langle \boldsymbol{F}, \boldsymbol{G} \rangle = \mathbf{0}.$$

A function $\boldsymbol{G} \in V_1$ is called multichannel *wavelet* for the MMRA if

$$W_j = \left\{ \mathbf{G} * \mathbf{c}(2^j \cdot) : \mathbf{c} \in \ell_2(\mathbb{Z})^{\mathbb{Z}_r} \right\}, \quad j \in \mathbb{N}_0,$$

and it is called an *orthonormal wavelet* if $\mathbf{G}$ is moreover orthonormal, i.e., if

$$\langle \mathbf{G}, \mathbf{G}(\cdot - j)\rangle = \delta_{0j}\mathbf{I}, \quad j \in \mathbb{N}_0$$

Suppose that $\boldsymbol{F}$ is an orthonormal $\boldsymbol{A}$-refinable matrix function, i.e. $\boldsymbol{A}^T\boldsymbol{A} = 2\boldsymbol{I}$, then there exists a bi-infinite matrix $B = [\boldsymbol{B}(j-2k) : j,\, k \in \mathbb{Z}]$ where

$$\mathbf{B} = \left(\mathbf{B}(k) \in \mathbb{R}^{\mathbb{Z}_r \times \mathbb{Z}_r} : k \in \mathbb{Z}\right) \in \ell_{00}^{\mathbb{Z}_r \times \mathbb{Z}_r}$$

such that $B^T A = 0$ and $B^T B = 2I$. Moreover this matrix B satisfies $AA^T + BB^T = 2I$. This matrix B is the key to the wavelet construction, in fact

$$\boldsymbol{G} := \boldsymbol{F} * \boldsymbol{B}(2\cdot) \in V_1.$$

To introduce a *fast wavelet transform* it is necessary to define, for any finitely supported matrix valued sequence $\boldsymbol{A} \in \ell_{00}^{\mathbb{Z} \times \mathbb{Z}_r}$, the *subdivision operator* $S_{\boldsymbol{A}}$ and the *decimation operator* $S^*_{\boldsymbol{A}}$:

***subdivision operator*:**

$$S_{\boldsymbol{A}}\boldsymbol{c} = \sum_{k \in \mathbb{Z}} \boldsymbol{A}(\cdot - 2k)\boldsymbol{c}(k) \quad \boldsymbol{c} \in \ell_2(\mathbb{Z})^{\mathbb{Z}_r}$$

***decimation operator*:**

$$S^*_{\boldsymbol{A}}\boldsymbol{c} = \sum_{j \in \mathbb{Z}} \boldsymbol{A}^T(j - 2\cdot)\boldsymbol{c}(j), \quad \boldsymbol{c} \in \ell_2(\mathbb{Z})^{\mathbb{Z}_r}$$

Then we can define the decomposition part of the pyramid scheme by setting

$$\boldsymbol{c}_{j-1} = \frac{1}{2} S^*_{\boldsymbol{A}} \boldsymbol{c}_j \quad \text{and} \quad \boldsymbol{d}_{j-1} = \frac{1}{2} S_{\boldsymbol{B}} \boldsymbol{c}_j \tag{2}$$

and the reconstruction part as

$$\boldsymbol{c}_j = S_{\boldsymbol{A}} \boldsymbol{c}_{j-1} + S_{\boldsymbol{B}} \boldsymbol{d}_{j-1} \tag{3}$$

3. Experimental Results

One of the most attractive features of multichannel wavelets is their effectiveness in the context of the signal compression and denoising. For this reason, we have experimented with the developed *full rank* filters in image compression and denoising based on *wavelet shrinkage*. Wavelet shrinkage, developed by *Donoho et al*[11,12] , selects the wavelet coefficients with significant energy by means *thresholding*. This technique will zero out many small coefficients, which results in efficient representation. There are two kinds of thresholding: *hard* and *soft* (Ref.13). Let I be the digital color image. The outputs entries $I^{hard}_{l,j,k}$ and $I^{soft}_{l,j,k}$ of the thresholding techniques with threshold δ are:

$$I^{hard}_{l,j,k} = \begin{cases} I_{l,j,k}, & if\ |I_{l,j,k}| > \delta \\ 0, & otherwise \end{cases}$$

$$I^{soft}_{l,j,k} = \begin{cases} sign(I_{l,j,k})(|I_{l,j,k}| - \delta), & if\ |I_{l,j,k}| > \delta \\ 0, & otherwise \end{cases}$$

Thresholding is lossy algorithm because the original signal cannot be reconstructed exactly starting from the processed signal.

We have developed denoising and compression algorithms based on wavelet shrinkage. In particular, we have applied the thresholding technique to multichannel wavelet coefficients. The performance of the multichannel wavelet scheme has been tested by means PSNR (Peak Signal to Noise Ratio) and WPSNR (Weight Peak Signal to Noise Ratio) values on the classical test images: *Lena*, *Baboon*, *Peppers*, *Lake*, *F16* and *House*. Instead, to value the compression score we have used the *energy ratio* in percentage defined by:

$$E = \frac{\left\|\hat{I}\right\|_2^2 \times 100}{\|I\|_2^2} \tag{4}$$

where I and $\hat{I}$ are respectively the original and compressed images.

Table 1. PSNR values of test images relative to the denoising processing by means soft (center) and hard (right) thresholding

Test image	**PSNR**		
	Noise	Den. ST	Den. HT
Lena	23.24	29.16	28.40
Peppers	22.23	28.86	27.62
Baboon	20.89	21.53	21.88
F16	20.47	27.43	26.26
Lake	21.42	26.10	26.03
House	21.41	27.37	26.72

In Table 1 and Table 2 there are explained the respectively PSNR and WPSNR values relative to the denoising technique. In the "*Noise*" column, we have inserted the PSNR (WPSNR) values relative to the original image and the image corrupted by noise. The "*Den. ST*"' ' and "*Den. HT*"' ' columns represent the PSNR (WPSNR) values relative to the original image and the

Table 2. WPSNR values of test images relative to the denoising processing by means soft (center) and hard (right) thresholding

Test image	WPSNR		
	Noise	Den. ST	Den. HT
Lena	38.10	38.27	38.55
Peppers	37.87	38.59	38.05
Baboon	33.57	36.53	35.10
F16	36.06	36.12	36.20
Lake	35.28	37.05	36.74
House	36.97	37.08	37.25

Table 3. PSNR corresponding to different value of compression putting to zero from 70% to 90% of wavelet coefficients by means hard thresholding

Test image	**PSNR**			
	70%	80%	85%	90%
Lena	35.7	21.1	17.1	14.0
Baboon	27.2	21.8	17.5	13.4
Peppers	39.0	30.2	25.0	20.3

image corrupted by noise after the denoising operation by means soft (*Den. ST*) and hard (*Den. HT*) thresholding. Fig. 1 represents an example of denoising operation by means hard and soft thresholding.

Table 4. WPSNR corresponding to different value of compression putting to zero from 70% to 90% of wavelet coefficients by means hard thresholding

Test image	**WPSNR**			
	70%	80%	85%	90%
Lena	51.3	29.3	25.3	22.1
Baboon	46.6	34.5	26.5	21.0
Peppers	51.1	40.1	34.5	29.2

(a) Original Image

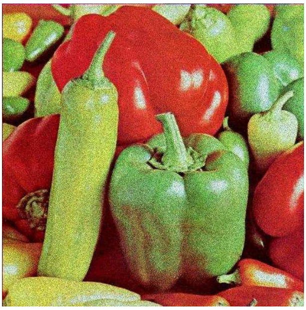

(b) Image corrupted by noise

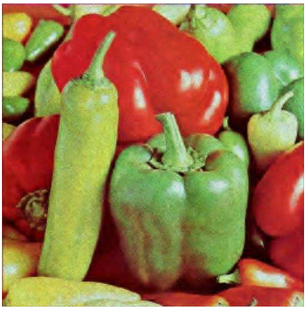

(c) Image corrupted by noise after soft thresholding

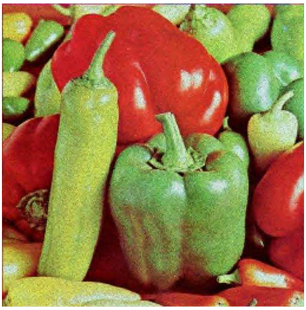

(d) Image corrupted by noise after hard thresholding

Fig. 1. Example of denoising operation by means hard and soft thresholding

(a) 70%

(b) 80%

(c) 85%

(d) 90%

Fig. 2. Example of compression *Lena* image by means hard thresholding putting to zero 70% (a), 80% (b), 85% (c) and 90% (d) of wavelet coefficients

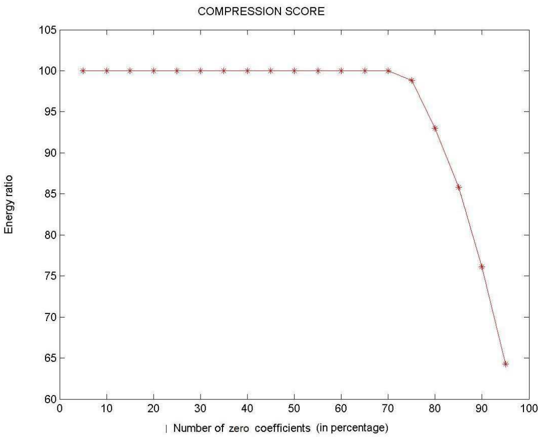

Fig. 3. Plot of energy ratio in percentage relative of *Lena* image

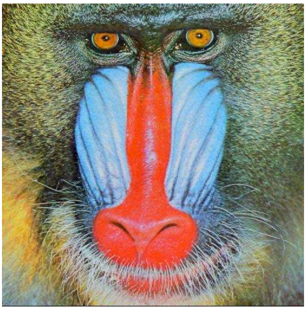

(a) 70%

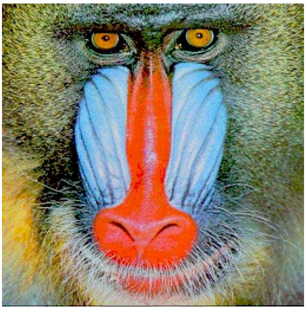

(b) 80%

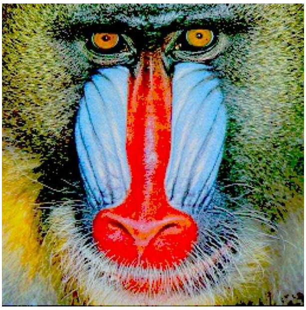

(c) 85%

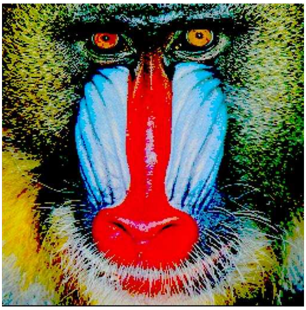

(d) 90%

Fig. 4. Example of compression of *Baboon* image by means hard thresholding putting to zero 70% (a), 80% (b), 85% (c) and 90% (d) of wavelet coefficients

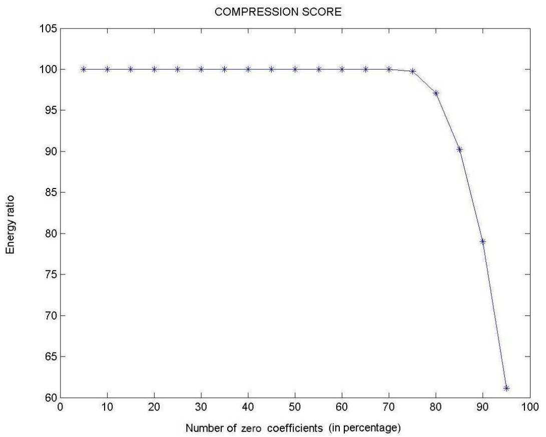

Fig. 5. Plot of energy ratio in percentage relative of *Baboon* image

APPLIED AND INDUSTRIAL MATHEMATICS IN ITALY III - Selected Contributions from the 9th SIMAI Conference

In Table 3 and Table 4 the PSNR and WPSNR values are presented corresponding to different values of compression respectively for Lena, Baboon and Peppers images. It can be observed that we obtain a good quality of compressed images putting to zero until 80% of coefficients (see Fig. 2 and Fig. 4). In Fig. 3 and Fig. 5 we have plotted the compression score of *Lena* and *Baboon* images corresponding to different values of thresholding obtained annihilating from 5% to 95% wavelet coefficients.

4. Conclusion

In this paper we investigated about the multichannel wavelets. We presented an overview about the mathematical theory showing a matrix wavelet approach which has the potential to form a convenient method for the analysis of vector-valued signals. Then we applied this vectorial approach on multichannel signal such as digital color images showing the results of a wide experimentation. *Lena*, *Baboon*, *Peppers*, *Lake*, *F16* and *House* images have been processed. PSNR and WPSNR values are illustrated relative to denoising and compression technique.
Next step is to build and test other multichannel wavelet based on several classes of *full rank* filters and to built an useful tool and a suitable software library for vectorial signal processing.

Acknowledgements

This work was supported by: PRA Projects of University of Messina and GNCS of INdAM.

References

1. J. Morlet, G. Arens, E. Fourgeau and D. Glard, *Geophysics* **47**, 203 (1982).
2. J. Morlet, G. Arens, E. Fourgeau and D. Giard, *Geophysics* **47**, 222 (1982).
3. L. Debnath, *Wavelet Transforms and Their Applications* (Birkhauser, 2002).
4. A. Cohen, *Numerical Analysis of Wavelet Methods* (Elsevier, 2003).
5. T. N. T. Goodman and S. L. Lee, *Transactions of the American Mathematical Society* **342**, 307 (1994).
6. G. Plonka and V. Strela, From wavelets to multiwavelets, in *Mathematical Methods for Curves and Surfaces II*, eds. M. Dahlem, T. Lyche and L. Shumaker (Vanderbilt University Press, 1998) pp. 1–25.
7. S. Bacchelli, M. Cotronei and T. Sauer, *Adv. Appl. Math.* **29**, 581 (2002).
8. S. Bacchelli, M. Cotronei and T.Sauer, *BIT 42* **2**, 231 (1998).
9. R. Gonzalez and R. Woods, *Digital Image Processing*, second edn. (Prentice Hall, 2001).

APPLIED AND INDUSTRIAL MATHEMATICS IN ITALY III - Selected Contributions from the 9th SIMAI Conference

10. C. Conti, M. Cotronei and T. Sauer, Full rank interpolatory vector subdivision schemes, in *Curve and Surface Fitting: Avignon 2006*, eds. A. Cohen, J. L. Merrien and L. S. Eds (Nashboro Press, Nashville, 2007).
11. D. L. Donoho and I. M. Johnstone, *Biometrika* **81**, 425 (1994).
12. D. L. Donoho and I. M. Johnstone, *Ann. Statist* **26**, 879 (1998).
13. G. Strang and T. Nguyen, *Wavelets and Filter Banks* (Wellesley-Cambridge Press,U.S., 1996).